

**EXTRACTION OF IODINE-131 (I-131) BY
SYNTHETIC AND NATURAL ANTIBACTERIAL
CARBON ADSORBENTS FOR CLINICAL
NUCLEAR MEDICINE WASTE MANAGEMENT**

ROSIDAH BINTI SUNAIWI

UNIVERSITI SAINS MALAYSIA

2023

**EXTRACTION OF IODINE-131 (I-131) BY
SYNTHETIC AND NATURAL ANTIBACTERIAL
CARBON ADSORBENTS FOR CLINICAL
NUCLEAR MEDICINE WASTE MANAGEMENT**

by

ROSIDAH BINTI SUNAIWI

**Thesis submitted in fulfilment of the requirements
for the degree of
Master of Science**

August 2023

ACKNOWLEDGEMENT

All praises to Allah SWT. With His mercy and blessing I have completed this dissertation entitled “Extraction of Iodine-131 (I-131) by Synthetic and Natural Antibacterial Carbon Adsorbents for Clinical Nuclear Medicine Waste Management” successfully. Many people have contributed to this research to fulfill the requirement for the master’s degree in health science (Medical Radiation) with Honours at Universiti Sains Malaysia Health Campus. I would like to thank Universiti Sains Malaysia Health Campus, School of Health Science and School of Health Science (PPSK) for providing a platform for me to carry out this research. Here I would like to express my sincere gratitude to my supervisor Dr. Mohammad Khairul Azhar Abdul Razab, who has given me useful advice and ideas as well as giving me excellent supervision throughout this research project. My sincere thanks to my Co-supervisor Dr. Norazlina Mat Nawi, Dr. Mohd Zahri Abdul Aziz and Dr. An'amt Mohamed Noor for their guidance helped me in the writing of this thesis. A special thanks to head of Nuclear, Radiotherapy and Oncology department, HUSM, Dr. Wan Fatimah Binti Wan Suhaimi, the radiopharmacist, and hot laboratory staff at Nuclear Medicine Department, HUSM who were so generous with their time and providing me platform to carried out my research project. I also like to extend my appreciation Mr. Nik Fakrudin Nik Ali and Miss Wan Norhasikin Wan Marizam of the School of Health Sciences, Universiti Sains Malaysia, for their help in obtaining the FESEM micrographs. I would like to dedicate my special appreciation to my beloved parents and Fara Hana binti Mohd Hadzuan for their encouragement and faithful help along the journey pursuing my master’s degree.

TABLE OF CONTENT

ACKNOWLEDGEMENT	ii
TABLE OF CONTENT	iii
LIST OF TABLES	vii
LIST OF FIGURES	viii
LIST OF SYMBOLS	xiv
LIST OF ABBRIVATIONS	xv
ABSTRAK	xviii
ABSTRACT	xx
CHAPTER 1 INTRODUCTION	1
1.1 Background of Study	1
1.2 Problem Statement	3
1.3 Significant of Study	4
1.4 Research Questions	5
1.5 Research Hypotheses	5
1.6 Research Objectives	5
1.6.1 General Objective	5
1.6.2 Specific Objectives	6
CHAPTER 2 LITERATURE REVIEW	7
2.1 Radioactive Iodine (RAI) Therapy	7

2.2 Radioactive Waste Management and Delay Tank Properties.....	9
2.3 Carbon-Based Adsorbents	12
2.3.1 Graphene Oxide Silver (GOAg).....	12
2.3.2 Bamboo Activated Carbon (BAC)	15
2.4 Antibacterial Properties of Carbon-Based Materials	19
2.4.1 Graphene Oxide Silver (GOAg).....	19
2.4.2 Bamboo Activated Carbon (BAC)	21
2.5 Materials Characterization Technique	22
2.5.1 Morphological Study Using Field Emission Scanning Electron Microscope (FESEM).....	22
2.5.2 Structural Analysis of Adsorbents Using X-ray Photoelectron Spectroscopy (XPS).....	24
2.5.3 Structural Analysis of Adsorbents Using Fourier Transform Infrared Spectroscopy (FTIR)	27
2.5.4 Structural Analysis of Adsorbents Using X-Ray Diffraction (XRD).....	29
2.6 Adsorption Mechanism of Carbon-Based Adsorbents.....	31
2.7 Particles and the Heavy Ion Transport Code System (PHITS) Simulation	33
CHAPTER 3 MATERIALS AND METHODS	37
3.1 Materials	37
3.2 Equipment	39
3.3 Methods.....	46

3.3.1 Synthesis of Graphene Oxide Silver (GOAg)	46
3.3.2 Preparation of Precursor	49
3.3.3 Synthesis of Bamboo Activated Carbon (BAC).....	50
3.3.4 Antibacterial Test of Adsorbents.....	51
3.3.5 Adsorbents Concentration Determination	52
3.3.6 Adsorbents Concentration Preparation.....	53
3.3.7 I-131 Radionuclide Extraction from Nuclear Medicine Radioactive Wastewater	55
3.3.8 Kinetic Study of Sediments	56
3.3.9 Characterization of Adsorbents and Sediments Using FESEM	57
3.3.10 Characterization of Adsorbents and Sediments Using FTIR	59
3.3.11 Elemental Binding Energy Analysis of Adsorbents and Sediments Using XPS	60
3.3.12 Structural Analysis of Adsorbents and Sediments Using XRD	63
3.3.13 Simulation of β^- Particle Distribution During Extraction Using PHITS	64
3.3.14 Post Data Collection (Disposal of Materials and Sample)	67
CHAPTER 4 RESULTS AND DISCUSSION.....	68
4.1 Kinetic Study of I-131 Extraction.....	68
4.1.1 GOAg:I-131.....	68

4.1.2 BAC:I-131	70
4.1.3 Percentage of Decay Rate.....	73
4.2 Characterization of Adsorbents and Sediments	75
4.2.1 Field Emission Scanning Electron Microscope (FESEM)	75
4.2.2 X-ray Photoelectron Spectroscopy (XPS) Analysis	85
4.2.3 Fourier Transformation Infrared Spectroscopy (FTIR).....	90
4.2.4 X-ray Diffraction (XRD) Analysis	94
4.3 Antibacterial Test of Adsorbents	97
4.4 Simulation of β^- Particle During Extraction Using PHITS	99
4.4.1 GOAg:I-131 and Control Group	99
4.4.2 BAC:I-131 and Control Group.....	102
CHAPTER 5 CONCLUSIONS	105
5.1 Conclusions.....	105
5.2 Recommendation of Future Works	106
REFERENCES	107
APPENDICES	

LIST OF TABLES

	Page
Table 3.1: Ratio of GOAg concentration preparation.....	54
Table 3.2: Ratio of BAC concentration preparation.	54
Table 4.2: Absorption peaks of GOAg and GOAg:I-131 with corresponding functional groups.....	91
Table 4.3: Absorption peaks of BAC and BAC:I-131 with corresponding functional groups.	93
Table 4.4: Peaks at 2θ value of GOAg and GOAg:I-131.	95
Table 4.5: Peaks at 2θ value of BAC and BAC:I-131.	97

LIST OF FIGURES

	Page
Figure 2.1: A typical delay tank design prior to the radioactive waste discharge from isolation wards (IAEA, 2013).....	11
Figure 2.2: The layout of delay tank room at Nuclear Medicine Department, Hospital Universiti Sains Malaysia (HUSM) where (A) is the area inside the delay tank room at 1 m distance from the delay tank, (B) is the door of the delay tan room, (C) is the public walking route (in front of the delay tank room) and (D) is the public walking route (lateral to the delay tank room) (Yusof, et al., 2016).	12
Figure 2.3: Molecular structure of GO (Zobir et al., 2018)	13
Figure 2.4: The chemical structure of a single sheet of GO (Stylianakis et al., 2019).....	14
Figure 2.5: Pictorial representation of GOAg (Kumari et al., 2020)	15
Figure 2.6: Morphological structure of BAC (Mistar et al., 2018).....	17
Figure 2.7: SEM micrograph image of coconut activated carbon (CAC) (Khuluk et al., 2019).....	18
Figure 2.8: Schematic mechanisms of GOAg antibacterial behaviors (Song et al., 2016).....	21
Figure 2.9: The electron beam column design of FESEM (Okano, 2018).	23
Figure 2.10: FESEM images from (A) Top-view of AgNP/GO composite paper; (B) Side-view of the cross sections of AgNP/GO composite paper (Bao et al., 2011).	24

Figure 2.11: SEM images (A) Microstructure of AC-Si and (B) Regular textured grooved structure of AC-Si (Su et al., 2020).	24
Figure 2.12: XPS survey spectra of GO and GO–AgNP (a) and high-resolution XPS spectra of Ag 3d of GO–AgNP (b) (Cobos et al., 2020).	26
Figure 2.13: High-resolution XPS spectrum of C 1s on GOAg surface (Zhu et al., 2021).	26
Figure 2.14: High-resolution XPS spectra of C1s peaks on BAC surface (Tan et al., 2011).	26
Figure 2.15: High-resolution XPS spectra of O 1s peaks on BAC surface (Liu et al., 2010).	27
Figure 2.16: FTIR spectrum of GOAg (Ahmad et al., 2021).	28
Figure 2.17: FTIR Spectra of BAC (Zawawi et al., 2017).....	29
Figure 2.18: XRD pattern of GO, AgNPs and GO-Ag nanocomposites (Kumari et al., 2020).....	30
Figure 2.19: XRD pattern of carbonized bamboo at 500 °C and 600 °C (Jena et al., 2021).	31
Figure 2.20: Schematic diagram of physisorption and chemisorption (Ayaz, 2022)	31
Figure 2. 21: Illustration of dipole-dipole interaction.....	32
Figure 2.22: Geometrical configuration of accelerator using PHITS simulation used for the J-PARC project in: (A) 2-D viewer and; (B) 3-D viewer; (C) interactive solid modeler SimpleGeo used for generating PHITS readable geometries in the GG format (Sato et al., 2015).....	35

Figure 2.23: PHITS application in: (A) accelerator design; (B) medical and radiation protection; (C) cosmic-ray research (Research Organization for Information Science and Technology, 2007).....	36
Figure 3.1: Chopped Bamboo trunk.....	37
Figure 3.2: Graphite powder	38
Figure 3.3: Magnetic stirrer	40
Figure 3.4: Homogenizer	40
Figure 3.5: (a) 15ml Hettich Centrifuge Rotina 38R, (b) 50ml Hettich Centrifuge Universal 32R.....	41
Figure 3.6: Furnace	42
Figure 3.7: Inspector Geiger-Mueller survey meter.....	42
Figure 3.8: Dose calibrator.....	43
Figure 3.9: Membrane filter	44
Figure 3.10: Centrifuge bottles	44
Figure 3.11: is FEI Quanta FEG 450 FESEM	44
Figure 3.12: FTIR BRUKER – TENSOR 27.....	45
Figure 3.13: Kratos Axis Ultra DLD - XPS.....	45
Figure 3.14: BRUKER D8 ADVANCE - XRD.....	46
Figure 3.15: Step of GO synthesis (Razab et al., 2022).....	48
Figure 3.16: Step of GOAg synthesis (Mohamed Noor et al., 2021).	49
Figure 3.17: Step of precursor preparation (JASNI et al., 2018).....	50
Figure 3.18: Synthesis of BAC (JASNI et al., 2018).....	51
Figure 3.19: Step of adsorbents concentration determination.....	53
Figure 3.20: Varies concentration of GOAg prepared in beakers	55

Figure 3.21: Varies concentration of BAC prepared in glass containers.....	55
Figure 3.22: Step of I-131 extraction.....	56
Figure 3.23: One of the sediment radioactivity measured using a dose calibrator. ...	57
Figure 3.24: Adsorbents and sediments before (A) and after gold coated (B).	57
Figure 3.25: LEICA EM SCD005 table-top sputter coater.....	58
Figure 3.26: Schematic diagram of generated signals when electrons bombarded the specimen's surface (Okano, 2018).	59
Figure 3.27: Gold coated adsorbents and sediments placed inside FESEM.	59
Figure 3.28: A drop of pure adsorbents or sediments placed on the sample surface.....	60
Figure 3.29: Sample holder of XPS.	62
Figure 3.30: Vacuum transport box with 2 parking load stage.	62
Figure 3.31: The sample is in position (load lock).	62
Figure 3.32: Step of XPS analysis.	63
Figure 3.33: Step of XRD analysis.	64
Figure 3.34: Illustration of dose calibrator during the measurement of radioactivity of sediments.	66
Figure 3.35: Constructed geometry of dose calibrator and sediment using PHITS... ..	66
Figure 4.1: The activity of I-131 clinical wastewater after being mixed with different concentrations of GOAg over days.	70
Figure 4.2: The activity of I-131 clinical wastewater after being mixed with different concentrations of BAC over days.....	72
Figure 4.3: Percentage of decay rate for GOAg:I-131 sediments and BAC:I-131 sediments at different concentrations over days.	74

Figure 4.4: R ² value of percentage of decay rate for GOAg:I-131 sediments and BAC:I-131 sediments at different concentrations over days.	74
Figure 4.5: FESEM image taken from GO at magnification: (A) 5,000, (B) 100,000 and (C) 100,000.	77
Figure 4.6: FESEM image taken from GOAg adsorbent at magnification: (A) 5,000; (B) 50,000.	79
Figure 4.7: FESEM image taken from I-131:GOAg sediment at magnification: (A)50,000; (B) 10,000; (C) 5,000.	81
Figure 4.8: FESEM image taken from BAC adsorbent at magnification: (A) 1,000; (B) 10,000.	83
Figure 4.9: FESEM image taken from I-131:BAC sediment at magnification: (A) 20,000; (B) 10,000.	84
Figure 4.10: Survey XPS spectrum of GOAg (A) and GOAg:I-131 (B).....	86
Figure 4.11: O 1s core level spectrum of GOAg (A) and GOAg:I-131 (B).....	86
Figure 4.12: C 1s core level spectrum of GOAg (A) and GOAg:I-131 (B).	87
Figure 4.13: Ag 3d core level spectrum on GOAg.	87
Figure 4.14: Survey XPS spectrum of BAC (A) and BAC:I-131 (B).	89
Figure 4.15: C 1s core level spectrum of BAC (A) and BAC:I-131 (B).	89
Figure 4.16: O 1s core level spectrum of BAC (A) and BAC:I-131 (B).	90
Figure 4.17: FTIR of pure GOAg before and after the adsorption process with I-131 wastewater.....	91
Figure 4.18: FTIR of BAC before and after the adsorption process with I-131 wastewater.....	93
Figure 4.19: XRD pattern of GOAg and GOAg:I-131.	95

Figure 4.20: XRD pattern of BAC and BAC:I-131.	97
Figure 4.21: GO, GOAg and BAC sample inhibition zone size for E. coli at (a) 1.0mg/ml, (b) 2.0mg/ml and 5.0mg/ml concentration.	98
Figure 4.22: Side view of β^- particle fluence of: (a) I-131 wastewater as a control group and GOAg:I-131 sediment at: (b) 1.0mg/ml; (c) 3.0mg/ml; (d) 5.0mg/ml concentration in dose calibrator.....	100
Figure 4.23: Energy distribution of β^- particle of: (a) I-131 wastewater as a control group and GOAg:I-131 sediment at: (b) 1.0mg/ml; (c) 3.0mg/ml; (d) 5.0mg/ml concentration in dose calibrator.....	101
Figure 4.24: Side view of β^- particle fluence of: (a) I-131 wastewater as a control group and BAC:I-131 sediment at: (b) 1.0mg/ml; (c) 3.0mg/ml; (d) 5.0mg/ml concentration in dose calibrator.....	103
Figure 4.25: Energy distribution of β^- particle of: (a) I-131 wastewater as a control group and BAC:I-131 sediment at: (b) 1.0mg/ml; (c) 3.0mg/ml; (d) 5.0mg/ml concentration in dose calibrator.	104

LIST OF SYMBOLS

%	percent
β^-	Beta minus
θ	Theta
\leq	Less than or equal to
$>$	More than
$<$	Less than
$^\circ$	Degree
$^\circ\text{C}$	Degree Celsius
\AA	Angstrom
μCi	microcurie
$\mu\text{Sv/hr}$	micro-Sievert per hour
eV	Electron volt
GeV/u	Gigaelectronvolts per Atomic Mass
GBq	Gigabecquerel
Hrs	Hours
keV	Kiloelectron volt
ml	milliliter
mg/ml	Milligram per milliliter
m ² /g	Meter square per gram
mCi	millicurie
MBq	Megabecquerel
mSv/hr	milli-Sievert per hour
rpm	Rotation per minute

LIST OF ABBRIVATIONS

I-131	Iodine-131
Tc-99m	Technetium-99m
Cu	Copper
Co ¹¹	Cobalt-11
Cd	Cadmium
Eu	Europium
Eu ¹¹	Europium-11
arsenate ¹²	Arsenate-12
U	Uranium
Sr	Strontium
Am	Americium
Ag ⁺	Silver ion
HCOONH ₄	Ammonium formate
AC	Activated carbon
ALARA	As low as reasonably achievable
BAC	Bamboo activated carbon
CrI	Crystallinity index
COOH, -COOH	Carboxyl group
C=O	Carbonyl group
COOH, -COOH	Carboxyl group
ROS	Reactive oxygen species
rh TSH	Recombinant thyroid stimulating hormone
C=C	Alkenes

<i>C. albicans</i>	Candida albicans
DNA	Deoxyribonucleic acid
<i>E. coli</i>	Escherichia coli
FTIR	Fourier Transform Infrared
	Field Emission Scanning
FESEM	Electron Microscopy
GO–AgNP	Graphene oxide-silver nanoparticle
GO	Graphene oxide
GOAg	Graphene oxide silver
GI tract	Gastrointestinal tract
H ₃ PO ₄	Phosphoric acid
H ₂ SO ₄	Sulphuric acid
KOH	Potassium hydroxide
NaI	Sodium iodide
NaOH	Sodium hydroxide
OH, O-H	Hydroxyl group
	Particle and Heavy Ion
PHITS	Transport Code System
RAI	Radioiodine ablation
	Radioactive iodine
RAIU test	uptake test
	Particle and Heavy Ion
PHITS	Transport Code System
<i>S. aureus</i>	Staphylococcus aureus
<i>S. epidermidis</i>	Staphylococcus epidermidis

XRD	X-ray Diffraction
XPS	X-ray Photo-electrons
ZnCl ₂	Zinc chloride

**PENGEKSTRAKAN IODIN-131 (I-131) MENGGUNAKAN PENJERAP
KARBON ANTIBAKTERIA SINTETIK DAN ASLI BAGI PENGURUSAN
SISA KLINIKAL PERUBATAN NUKLEAR**

ABSTRAK

Pesakit yang menjalani dos tinggi bagi terapi ablasi radioiodin (RAI) perlu diasingkan di wad yang direka khas di jabatan perubatan nuklear (Lian, 2013). Sehubungan dengan itu, sisa kumbahan daripada pesakit tersebut dikategorikan sebagai sisa radioaktif. Sejumlah besar kumbahan radioaktif terhasil apabila lebih banyak terapi radionuklid yang melibatkan radioaktiviti yang tinggi dilaksanakan. Air kumbahan radioaktif perlu disimpan dalam tangki tangguh (sistem kumbahan bawah tanah) sehingga radioaktiviti menurun ke had yang ditetapkan ($<1.2 \mu\text{Ci}$ seliter) sebelum dibuang ke pembetung awam (IAEA, 2000). Tangki tangguh secara tidak langsung menghadkan bilangan kemasukan pesakit kerana isipadu tangki tangguh yang terhad dan tangki tangguh juga mempunyai pelepasan berkala. Oleh itu, kajian ini bertujuan mencadangkan penjerap antibakteria alternatif bagi pengekstrakan I-131 daripada air sisa kumbahan klinikal radioaktif di jabatan perubatan nuklear dengan menggunakan grafin oksida argentum (GOAg) dan 'bamboo activated carbon' (BAC), bahan berasaskan karbon yang mesra alam dan pada masa yang sama merupakan penjerap karbon antibakteria yang sintetik dan semula jadi. Sampel air sisa kumbahan klinikal radioaktif dari tangki tangguh akan dicampur dengan GOAg dan BAC pada kepekatan 1, 2, 3, 4 dan 5 mg/ml sebelum ditapis menggunakan penapis membran. Peratusan kadar pereputan untuk kedua-dua bahan berasaskan

karbon pada kepekatan 5 mg/ml jauh lebih tinggi berbanding mana-mana kepekatan. Bahan berasaskan karbon yang telah disintesis dan sedimennya yang terbentuk pada penapis membran dianalisis menggunakan; FESEM untuk analisis morfologi; spektrum XPS bagi C1s penjerap menunjukkan puncak keamatan: (a) $C=C$ dan $C-C$ bagi GOAg dan sedimennya; (b) $C-C$, $C=O$ dan peralihan $\pi-\pi^*$ bagi BAC dan sedimennya; spektrum FTIR menunjukkan penjerap pelbagai kumpulan berfungsi; (a) $C=C$, $C=O$ dan $C-O-C$ bagi GOAg dan sedimennya; (b) $C=C$, $C-C$ dan $C-O$ bagi BAC dan sedimennya; penghabluran setiap penjerap yang dianalisis menggunakan XRD mempamerkan corak puncak XRD pada nilai 2θ yang dikaitkan dengan; (a) satah difraksi (002), (220) satah kristalografi, (111) satah Ag_2O dan (200) satah kristalografi bagi GOAg dan sedimennya; (b) satah (002) dan (100) bagi BAC dan sedimennya. Simulasi zarah beta yang tinggal semasa proses penyahcemaran I-131 dijalankan menggunakan PHITS. Penemuan kajian ini menunjukkan potensi bahan penjerap boleh diganti dan juga penapisan untuk pengekstrakan radionuklid daripada air sisa radioaktif dalam perkhidmatan perubatan nuklear. Tambahan pula, boleh juga berfungsi sebagai penyelesaian alternatif peningkatan had kemasukan pesakit sedi ada di Hospital Universiti Sains Malaysia, Kubang Kerian, Kelantan.

**EXTRACTION OF IODINE-131 (I-131) BY SYNTHETIC AND NATURAL
ANTIBACTERIAL CARBON ADSORBENTS FOR CLINICAL NUCLEAR
MEDICINE WASTE MANAGEMENT**

ABSTRACT

Patients undergoing high-dose radioiodine ablation (RAI) therapy need to be isolated in the specially designed ward at the nuclear medicine department (Lian, 2013). Thus, excreta from those patients are considered radioactive waste. A large amount of radioactive sewage is produced as more high-activity radionuclide therapy is implemented. The radioactive wastewater had to be stored in a delay tank until the radioactivity decayed below the legally established acceptable limit ($<1.2\mu$ Ci/L) before being discharged into the public sewer (IAEA, 2000). A delay tank indirectly limits the number of patient admissions due to its limited volume size and periodical clearance. Thus, this study's purpose is to propose an alternative antibacterial adsorbent for I-131 extraction from clinical radioactive wastewater at the nuclear medicine department by using graphene oxide/silver (GOAg), and bamboo activated carbon (BAC), environmentally friendly carbon-based adsorbent materials and serve as synthetic and natural antibacterial carbon adsorbent. Radioactive clinical wastewater samples from a delay tank are mixed with adsorbents at concentrations 1, 2, 3, 4 and 5 mg/ml before being filtered using a membrane filter. The percentage of decay rate for both carbon-based materials at 5 mg/ml was significantly higher than any concentrations which is 84.05% for GOAg:I-131 and 77.78% for BAC:I-131. The synthesized carbon-based materials and its sediments formed on

the membrane filter were analyzed using; FESEM for morphological analysis; XPS spectrum for C1s of adsorbents show intensity peaks of: (a) $C=C$ and $C-C$ for GOAg and its sediments; (b) $C-C$, $C=O$ and $\pi-\pi^*$ transitions for BAC and its sediments; FTIR spectra revealed various functional groups of adsorbents; (a) $C=C$, $C=O$ and $C-O-C$ for GOAg and its sediments; (b) $C=C$, $C-C$ and $C-O$ for BAC and its sediments; crystalline of adsorbents analyzed using XRD, the XRD pattern exhibit peaks at 2θ value that attributed to: (a) (002) diffraction plane, (220) crystallographic plane, (111) plane of Ag_2O and (200) crystallographic plane in GOAg and its sediments; (b) (002) and (100) plane in BAC and its sediments. Estimation of remaining beta particles during the decontamination of I-131 was carried out using PHITS. The finding of this study can indicate the potential for the innovation of replaceable adsorbent material and filtration for radionuclide extractions from radioactive wastewater in nuclear medicine services. Furthermore, it can also serve as an alternative solution to increase the admission limit for existing patients at Hospital Universiti Sains Malaysia, Kubang Kerian, Kelantan.

CHAPTER 1

INTRODUCTION

1.1 Background of Study

The nuclear medicine department is one of the facilities that provide diagnostic and therapeutic services for patients through the aid of radiopharmaceuticals (I-131 and Tc-99m) which will be administered into the patient's body orally or intravenously (Siti, 2019). Management of radionuclides in the nuclear medicine department required a special procedure in terms of radiation protection, especially in radioactive waste management. This is needed due to the production of massive radioactive clinical wastewater from the patient's body after radioiodine treatment. Thus, good management and systematic disposal of clinical radioactive waste in nuclear medicine departments have always been a concern for both health institutions and regulatory authorities (Ravichandran et al., 2011).

In radioiodine therapy, I-131 radionuclide (beta particle emanations) is widely used to destroy any remaining cancerous thyroid tissue after a thyroidectomy procedure and treat residual and persistent disease (Maiden, 2017). The patient is isolated in the specially designed ward for a few days until the radiation level from the patient body falls below 50 uSv/hr at a 1-meter distance before being discharged (Ministry of Health Malaysia, 2017). Thus, the radioactive waste from the patient's body (urine and feces) will go through a sewage system with a specially designed delay tank and be stored. Before clinical radioactive waste can be released into the ordinary sewage system, delay tank is used as a temporary storage system to reduce the activity of clinical radioactive wastewater at a certain level (Razab et al., 2020). This is known as the delay and decay

method (Amaral & Michaud, 2001). The delay tank is also used to prevent contamination or leakage of clinical waste from the patient's body, mostly via the urinary and gastrointestinal systems (Yusof et al., 2016). However, radioactive waste from the diagnostic patient's body will also go into the delay tank, increasing the therapeutic I-131 waste volume in the isolation wards, thus increasing the dilution factor (Ravichandran et al., 2011).

Activated carbon (AC) is very popular among researchers because it focuses on recycling agricultural waste into beneficial usage (Rasat et al., 2016). This environmentally friendly approach aims to reduce the impact of waste to the environment. Furthermore, the application of waste to wealth concept would allow the agricultural byproducts which do not have any economic value. In this study, bamboo trunks were used. Large amount of bamboo left over from the construction and woodworking industries. Thus, the leaf, trunk, and root parts can be used in bamboo activated carbon (BAC) production. BAC has unique properties, such as highly porous carbonaceous material, with an elevated internal surface area and functional groups. These properties make BAC have high adsorption affinity and faster adsorption rate for heavy metal ions (Waji, 2018). BAC also has natural antibacterial properties. It is concluded that the antibacterial compound of bamboo located in lignin stems from the aromatic and phenolic functional groups in lignin (suggestion from FTIR results). Besides, a 100% sterilization rate against strong bacteria such as E. coli can be achieved at the lowest concentration (5%) of bamboo extract in water (Afrin et al., 2012). Therefore, the natural antibacterial compound of bamboo located in lignin makes it a priority for wastewater/contaminated area cleaning.

Hybrid material formation and exploration have been among the most interesting fields lately (Zin et al., 2020). A combination of graphene oxide (GO) and silver (Ag) nanoparticles as a synthetic adsorbent and BAC as a natural adsorbent is believed that it could contribute to health, agriculture, and technology sector, particularly in improving antibacterial performance and radionuclide removal. GO has attracted multidisciplinary interests due to its unique properties, such as physical stability, chemical stability, high specific surface area, abundant oxygen-containing functional groups, electron mobility and heat transfer (Giannakoudakis & Bandosz, 2019). These properties made it possible for GO to form homogeneous suspensions in water between the negatively charged functional groups of GO and positively charged heavy metal ions through electrostatic interaction (Romanchuk et al., 2013). GO demonstrates high sorption affinity for the most toxic radionuclides from various solutions and is much more effective in removing actinides from liquid nuclear waste (Concklin, 2014). In contrast, Ag nanoparticles have a high specific surface area and high physiochemical properties (Chook et al., 2012). These properties make it an alluring material to be used in the pharmaceutical and antibacterial fields, and Ag nanoparticles also show good performance towards its function (Zin et al., 2020). However, the adsorption interactions of GOAg and BAC with I-131 in radioactive clinical wastewater still not been comprehensively studied.

1.2 Problem Statement

The delay and decay method of radioactive waste management indirectly restricts the number of patient admission due to the limited volume size of the delay tank (relatively limited and non-strategic location of the tank) and have periodical clearance. Wastewater from the delay tank can only be discharged into the normal sewage system

when the radioactivity is less than 1.2 μCi per liter (Khan et al., 2010). Hence, it remains a challenge to achieve effective and economical methods for radioactive wastewater management in radioiodine therapy (Efremenkoy, 2000). Moreover, radioactive waste from the diagnostic patient's body will also go into the delay tank, contributing to waste volume (Ravichandran et al., 2011). The delay tank cannot support and bear the weight of large quantities of radioactive wastewater.

1.3 Significant of Study

The easier way to overcome this problem is to extract the contaminated radioactive clinical wastewater from the delay tank using a special adsorbent material and transform it into a solid form for fast disposal via the concentration and contain method. The concentration and contain method of radioactive waste management is more practical than the delay and decay method when space availability is limited. This method is usually used for high-activity radioactive solid waste with long half-lives (Kahn et al., 2010). Thus, it is practical for the re-solidification of clinical wastewater in nuclear medicine. Furthermore, the concentration and contain method is suitable for rapid radioactive disposal due to its uncomplex handling procedure. The solidified clinical radioactive waste can be easily sealed in a proper labeled lead container, and any radioactive spillage can be avoided. Hence, optimum radiation protection principle can be applied. This research proposed to use synthetic graphene oxide/silver (GOAg), and natural bamboo activated carbon (BAC) based materials as super adsorbents in extracting the clinical radioactive wastewater from a delay tank for aseptic aspect and as a solution to patient admission limitation. This study also may become one of the contributions, ideas or supportive explanations to invent a replaceable adsorbent material

and filter for radionuclides extractions from radioactive wastewater in nuclear medicine services.

1.4 Research Questions

- 1.4.1 Do synthetic carbon-based adsorbent graphene oxide/silver (GOAg), and natural antibacterial carbon-based adsorbent bamboo activated carbon (BAC) accelerate the decay rate of radioactive clinical wastewater from the delay tank?
- 1.4.2 Which prepared carbon-based adsorbents adsorb radioactive clinical wastewater more efficiently?
- 1.4.3 Is the radioactivity of clinical wastewater from the Nuclear Medicine Department of Hospital Universiti Sains Malaysia (HUSM) able to reduce by carbon-based adsorbents during the decontamination process?

1.5 Research Hypotheses

- 1.5.1 There are significant differences in I-131 extraction from clinical radioactive wastewater in a delay tank using Graphene oxide/silver (GOAg) and BAC as synthetic and natural antibacterial carbon adsorbents that vary in concentration.
- 1.5.2 Actual measurement using well counter and theoretical calculation of radioactivity using the Beer-Lambert equation might be different due to adsorption interactions.

1.6 Research Objectives

1.6.1 General Objective

To design an alternative antibacterial adsorbent for I-131 extraction from clinical radioactive wastewater.

1.6.2 Specific Objectives

- I) To synthesize and characterize graphene oxide (GO), GOAg and bamboo activated carbon (BAC) as synthetic and natural antibacterial carbon adsorbents.
- II) To determine the kinetic radioactivity of clinical wastewater after extraction using carbon-based materials.
- III) To characterize the extraction of clinical radioactive wastewater using FESEM, FTIR, XPS, and XRD.
- IV) To simulate β^- particle distribution during the extraction process using a heavy-ion transport code system (PHITS).

CHAPTER 2

LITERATURE REVIEW

2.1 Radioactive Iodine (RAI) Therapy

Radioactive iodine (RAI) therapy is a type of radiation therapy that uses radioactive iodine-131 (I-131) to remove or destroy any residual cancer tissue that remains after a thyroidectomy (Nostrand, 2012). I-131 emits both beta minus (β^-) particles (606 keV) for therapeutic purposes and 346 keV gamma rays for diagnostic purposes, with a physical half-life of about 8.01 days (Mody, et. al, 2015). I-131 is used to treat thyroid cancer and hyperthyroidism at the nuclear medicine department (KOCA et al., 2021). In addition, routinely administered as a radiopharmaceutical in the form of sodium iodide (NaI) for both the diagnosis and treatment of thyroid disease (Suksompong et al., 2021). There are two types of RAI therapy which are low and high doses of I-131 that are prescribed by the medical physicist and the doctor. The radioactivity of I-131 prescribed in low-dose RAI therapy is ≤ 30 mCi (≤ 1100 MBq) for each therapy. While for high-dose RAI therapy, the radioactivity prescribed is greater than 30 mCi (1100 MBq) for each therapy (Medical Radiation Surveillance Division Ministry of Health Malaysia, 2017). Researchers discovered that high RAI doses therapy > 150 mCi for patients (in a propensity-matched cohort) with differentiated thyroid cancers with high-risk features were associated with a lower recurrence rate (Gray et al., 2019).

The dose selection to be administered is based on the estimated size of the thyroid gland or residual functioning tissue present and the results of a 24-hour RAIU

test (Meier et al., 2002). Orally administrated I-131 was quickly absorbed into the bloodstream in the digestive system (Savage et al., 2015). I-131 causes acute cell death by penetrating the thyroid cells through the sodium iodide transporters and emitting short-wavelength of β -rays. After a single dose of I-131, several tests are conducted to validate a successful I-131 treatment. Two to eight days after the treatment, a whole-body scan is carried out to confirm the I-131 uptake and a follow-up scan is normally carried out six to twelve months later. The treatment is successful when the follow-up scan reveals less than 0.1% I-131 uptake in the thyroid bed as well as a low level of stimulated thyroglobulin. An empty thyroid bed should be visible on a neck ultrasound, without any new growths or extensions (Nguyen et al., 2015).

Before beginning the therapy, the patient must have complied with some important instructions for the therapy to work, such as patients have to discontinue iodide-containing medications for a sufficient amount of time prior to therapy and preparations to avoid any potential effects on the thyroid tissue's ability to accumulate iodide or take recombinant thyroid stimulating hormone (rh TSH) which will maximizing thyroid gland uptake while minimizing the radiation dose to other parts of the body and most experts recommend a low iodine diet for one to two weeks before the treatment to improve radioiodine uptake. Pregnancy tests must always be performed on female patients who may be pregnant, ideally within 24 hours of treatment. In addition, women who have to breastfeeding must be counselled to stop breastfeeding and therapy must be postponed until lactation ends to minimize radiation dose to the breast (Silberstein et al., 2012).

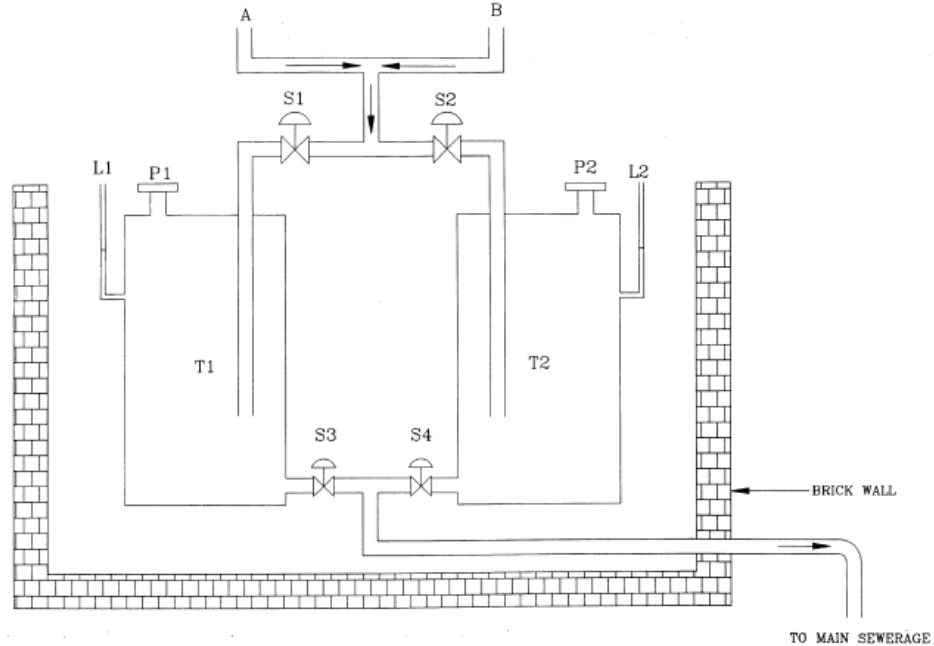
For low-dose I-131 therapy, the patient is allowed to return home, while the patient that undergoes high-dose therapy needs to be admitted to the isolation ward at the nuclear medicine department until get permission to release (IAEA, 2009). Radioactive I-131 with activities ranging from 1.85 GBq to 7.0 GBq are used for the administration to treat patients with differentiated thyroid cancer. The patient needs to be awarded for a few days until the measured radioactivity in their body reaches a permitted level to be discharged, which is $<10 \mu\text{Sv/h}$ at 1 meter (Al Aamri et al., 2019). Those at risk of radiation exposure when the patient is hospitalized following the therapy are hospital staff or caretakers who are well-trained. Once the patient is discharged, their family members, including children and expectant mothers become the groups most at risk. Additionally, they could be people they meet in public places and events or even their neighbors, house guests and coworkers (IAEA, 2009).

2.2 Radioactive Waste Management and Delay Tank Properties

Radioisotopes are used for diagnostic and therapeutic purposes in the majority of tertiary care hospitals. The safe disposal of radioactive waste is essential to hospital waste management. The aim of radioactive waste management to ensure that radiation exposure to the general public, radiation workers, patients, and the environment does not surpass the prescribed safe limits. The basic principles for radiation protection in radioactive hospital waste management that need to be followed are the justification of practice (ensure that the benefits outweigh the risks), optimization of practice (ensure that individual dose and the number of people exposed are as low as reasonably achievable, ALARA) and dose limitation (Khan et al., 2010).

It is crucial to design an effective system for managing biomedical radioactive waste in handling radioisotopes in medical or health care facilities. Most radionuclides used in nuclear medicine departments have short half-life (IAEA, 2000). The main radionuclides used at Nuclear Medicine Department, Hospital Universiti Sains Malaysia (HUSM) are technetium-99m (Tc-99m) and I-131 with half-lives 6 hours and 8 days, respectively. Hospitals that administer large quantities of I-131 for therapeutic purposes have delay tanks for secure storage and safe disposal of radioactive effluents from isolated patient excretion in the isolation ward. Moreover, approximately 80% of the administered I-131 is excreted in the urine (Suksompong et al., 2021).

Contaminated radioactive wastewater in the delay tank is stored before it can be discharged into a normal sewage system when the radioactivity in the delay tank is less than 1.2 μCi per liter (Kahn et al., 2010). It is known as the delay and decay method, the most popular method in handling radioactive wastewater. An appropriate capacity of the delay tank should be determined based on the anticipated daily release of effluents from the isolated ward, which allows the activity to decay (correspond to 6–8 half-lives) before discharge into the public sewage system. Moreover, it assures that approximately 1% of the initial activity remains in the tank when it is released into the public sewage system. In addition, two tanks with a capacity of approximately 5,000 liters each may be sufficient for a two-bed isolation ward. The delay tank should comply with these requirements: it should be leak-proof, corrosion-resistant and have smooth interior surfaces. To avoid effluent backflow, the tanks' outlets should be positioned higher than the main sewerage line (IAEA, 2000). A typical delay tank design is shown in Figure 2.1.



- P1, P2 – Provisions for collecting samples / inserting probe for estimating radioactivity concentration;
- S1, S2 – Inlet gas valves;
- S3, S4 – Outlet valves;
- L1, L2 – Fluids level indicators;
- T1, T2 – Storage tanks (preferably below ground level);
- A, B – Outlets of toilets of I-131 therapy patients wards.

Figure 2.1: A typical delay tank design prior to the radioactive waste discharge from isolation wards (IAEA, 2013).

The layout of delay tank room at Nuclear Medicine Department, Hospital Universiti Sains Malaysia (HUSM) is shown in Figure 2.2. There are two tanks with a capacity of 3,568 liters each at the Nuclear Medicine Department, HUSM, for a two-bed isolation ward, which is less than the recommended capacity of the delay tank, as mentioned above. Thus, indirectly restricts the number of patient admission due to the relatively limited volume size of the delay tank. Therefore, only 4 patients were treated in a month, making it 20 patients can be treated in a cycle (5 months) before the delay tank pump out. The delay tank has periodical clearance, which is on the fifth month (forth week), as shown in Appendix C. Each cycle takes about a week to empty the

delay tank, which is considered long. Therefore, the findings of this study may help in serving more patients in a shorter time period.

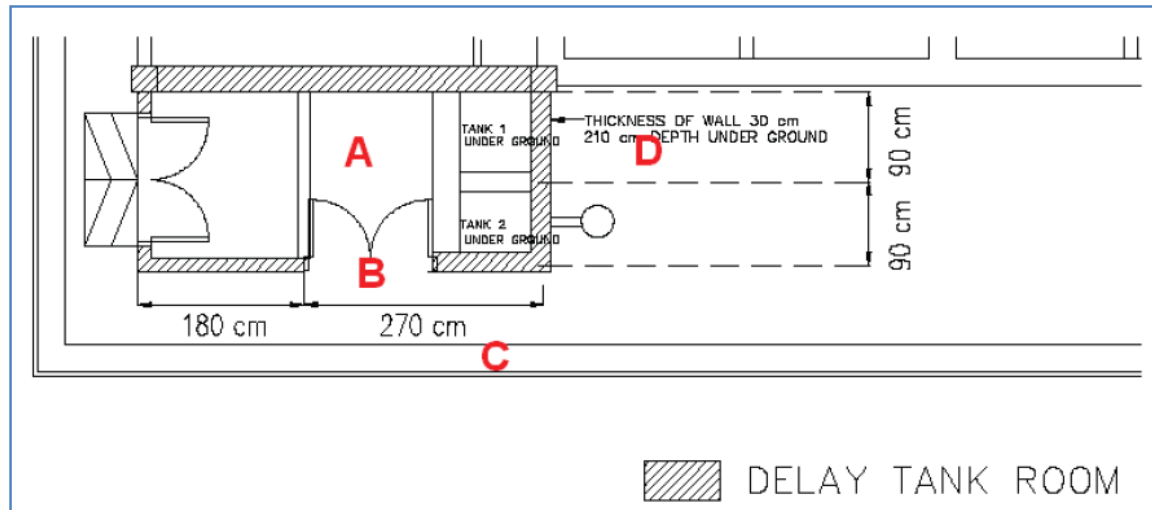


Figure 2.2: The layout of delay tank room at Nuclear Medicine Department, Hospital Universiti Sains Malaysia (HUSM) where (A) is the area inside the delay tank room at 1 m distance from the delay tank, (B) is the door of the delay tank room, (C) is the public walking route (in front of the delay tank room) and (D) is the public walking route (lateral to the delay tank room) (Yusof, et al., 2016).

2.3 Carbon-Based Adsorbents

2.3.1 Graphene Oxide Silver (GOAg)

Graphene oxide (GO) is a mono-layer structure comprising sp^2 hybridized carbon atoms and various oxygen-containing surface functional groups. GO has various unique properties, which are physical stability, chemical stability, high specific surface area, electron mobility and heat transfer (Giannakoudakis & Badosz, 2019). Furthermore, GO has hydrophobic (nonpolar) and hydrophilic (polar) regions, also referred to as amphiphilic GO. This makes the GO create stable suspension and exhibit excellent adsorption capacity when dispersed in liquids (Romanchuk et al., 2013). In addition, the presence of oxygen functional groups on the surface of graphene results in enhanced layer separation and improved hydrophilicity (Figure 2.3) (Zobir et al., 2018).

GO has rich functional groups such as hydroxyl (OH), epoxy and carboxyl (COOH) moieties, as shown in Figure 2.4. These surface moieties are able to form strong surface complexes with cations and anions in radionuclides. GO offers excellent removal of Cu, Co¹⁰, Cd, Eu¹¹, arsenate¹² and organic solvents (Concklin, 2014). Besides, GO has the ability to coagulate easily with cations in radionuclides. Thus, this makes it a promising new material for radionuclide removal (Tour et al., 2016). In addition, GO also has high accessible surface areas resulting in fast sorption kinetics is crucial for practical applications of GO in the removal of cationic impurities. GO lack of internal surfaces normally contributes to the slow diffusion kinetics in cation-sorbent interactions. According to the sorption isotherms, GO has a high sorption capacity for U, Sr, Am, and Eu cations (Naguib, 2016). Based on Concklin (2014) and Romanchuk et al. (2013), GO demonstrates high sorption affinity for the most toxic radionuclides from various solutions and is effective in removing actinides from liquid nuclear waste.

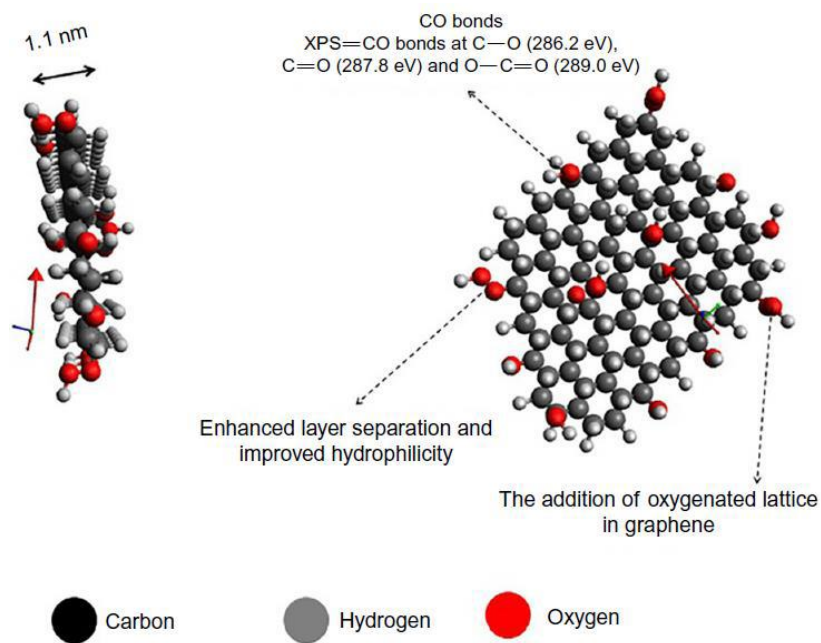


Figure 2.3: Molecular structure of GO (Zobir et al., 2018)

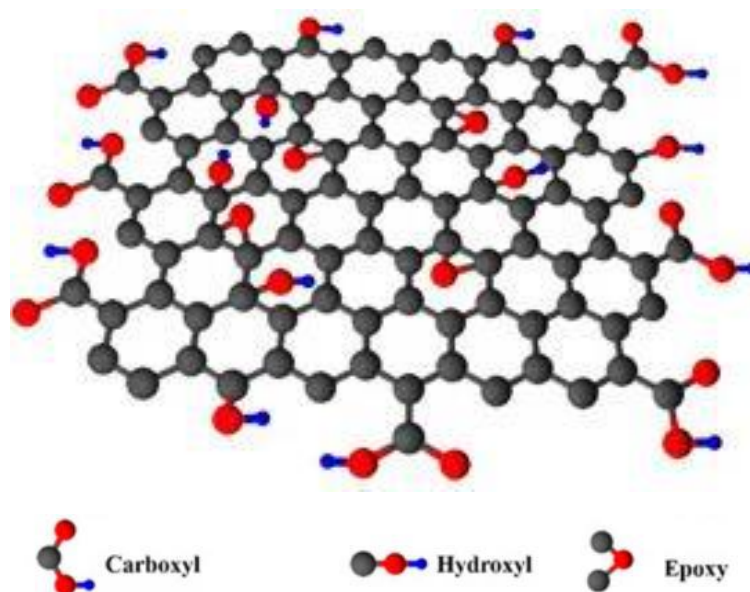


Figure 2.4: The chemical structure of a single sheet of GO (Stylianakis et al., 2019)

Surface functionalization of GO has numerous opportunities for its use in nanocomposite materials development. Moreover, the nanocomposite enhances the properties of GO. Silver (Ag) is the most conductive and reactive material among all transition elements (Kumari et al., 2020). Hybrid material formation and exploration have been one of the most interesting fields lately. AgNPs have recently gained a lot of attention in antibacterial applications due to their antibacterial properties (Zin et al., 2020). The synthesis of GO–AgNP hybrids as synthetic adsorbents are believed to contribute to health, agriculture, and technology, particularly in improving antibacterial performance and radionuclide removal. Ag was dispersed on the GO surface and intercalated between nanosheets to study the electrochemical properties of samples. In addition, Ag-doped GO have favorable properties of low resistance and good dispersion (Kumari et al., 2020).

The formation mechanism of GOAg nanocomposites is as follows: the GO contains numerous oxygen functional groups that constitute a significant amount of binding sites for Ag^+ . Positively charged Ag^+ in an aqueous solution was easily captured by negatively charged GO due to electrostatic interaction, which further promotes the antibacterial activity of GOAg (Zhu et al., 2013). Following that, silver ions were reduced in situ with HCOONH_4 and AgNPs were uniformly distributed on the surface of GO sheets, forming a stable GOAg nanocomposite. Furthermore, AgNPs-GO interaction can be attributed to physisorption, electrostatic binding and charge-transfer interactions (Song et al., 2016).

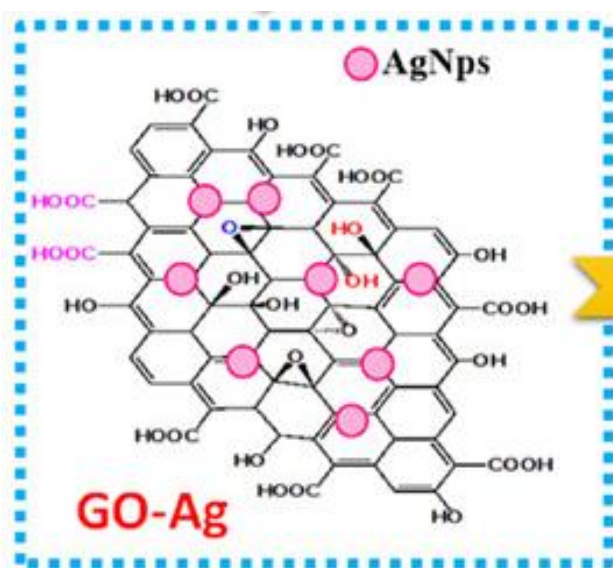


Figure 2.5: Pictorial representation of GOAg (Kumari et al., 2020)

2.3.2 Bamboo Activated Carbon (BAC)

Activated carbon has a wide range of applications but is hindered by its high cost. Bamboo is an abundantly available and inexpensive natural resource that has been used as an alternative source for producing activated carbon (Ma et al., 2018). It has a great adsorbent and is classified as an amorphous carbon for its high porosity and

specific surface area (Ip, Barford, & McKay, 2008). Pore size distribution defines the porous structure of activated carbon, which is classified into three types, according to the International Union of Pure and Applied Chemistry (IUPA) (Chien et al., 2011). This pore size distribution directly influences the diffusion rate of an adsorbate to the adsorption sites. While the adsorption capacity of adsorbate is defined by the specific surface area and pore volume of activated carbon (Phothong et al., 2021). The first type of porous structure has small pores that allow one or two molecules to be adsorbed per pore with strong interaction between the pore wall and the adsorbed molecules. The second type has mesopores that might exhibit capillary phenomena and hysteresis loop characteristics under relatively high pressure (Hu et al., 2001). The third type includes macroporal sizes with a relatively lower surface area to porosity ratio. Even though particles with macropores have a low specific surface area, they can serve as channels between mesopores and micropores (Chien et al., 2011).

According to previous studies, the specific surface area analysis using Brunauer-Emmett-Teller (BET) specific surface area of BAC ranges from 1196.30 m²/g to 3208 m²/g (Santana et al., 2017; Horikawa, et al., 2010; Ma, et al., 2014; Zhao, et al., 2016). Activated carbon contains heteroatoms such as oxygen, nitrogen, hydrogen and sulphur, which can react with the oxidizing agent during the activation process, resulting in the formation of various surface functionalities on the activated carbon surface. Furthermore, formation of surface functional groups of activated carbon depends on the raw materials used and preparation conditions which are the carbonization and the activation conditions that will aid in selecting the best-activated carbon for a specific application (Phothong et al., 2021). Lactones, ketones, carboxylic anhydrides, quinine

structure and aromatic ring, are the main surface functional groups found on BAC (BAC preparation _KOH). In addition, surface functional groups of BAC that are prepared through KOH activation are O-H, C-O, C=O and C=C (Zawawi et al., 2018).

In addition, BAC is the most widely used adsorbent for removing pollutants from wastewater due to its high adsorption capacity, broad applicability and easy availability (Kim, Kim, & Yamamoto, 2008). Activated carbon has been effectively used to remove a wide range of dyes from wastewater with high capacity (Ip, Barford, & McKay, 2008). Thus, BAC was found to be suitable for the removal of large dye molecules while tough in separating a thick molecule with a hydrophilic functional group. Unlike conventional activated carbon derived from coconut shells or coal, BAC has relatively large pores that are suitable for large molecule adsorption (Figure 2.6 & 2.7) (Kim et al., 2008). Moreover, it has been amply demonstrated that BAC is a far superior adsorber to coconut shell-activated carbon with 98.90% efficiency in absorbing the dye from the aqueous solution, which is significantly influenced by the amount of adsorbents, initial coloration concentration, pH value, temperature, contact time and agitation speeds (Bokil et al., 2020).

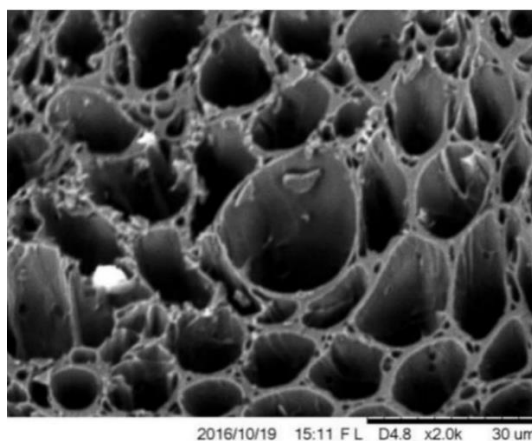


Figure 2.6: Morphological structure of BAC (Mistar et al., 2018)

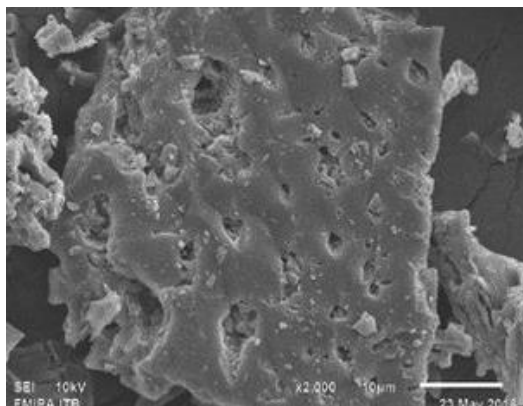


Figure 2.7: SEM micrograph image of coconut activated carbon (CAC) (Khuluk et al., 2019)

Bamboo carbon is typically prepared through chemical or physical activation under various conditions to enhance the pore structure. In physical activation, bamboo needs to be enriched with carbon content as well as create an initial porosity through the carbonization process (Mahanim et al., 2011). Furthermore, the carbonization process will remove the bulk of volatile matter, which results in char. Activating agents such as carbon oxide, steam, air or a combination of these agents can be used for physical activation. It is a complex, heterogeneous process that involves the transport of gas agents to the surface of the sample, diffusion into the pores, sorption on the pore surface and reaction with the carbon component of activating agents along with desorption of the reaction products and their diffusion into the atmosphere (Zhou et al., 2018). In chemical activation, the precursor is impregnated with certain chemicals such as H_3PO_4 , H_2SO_4 , ZnCl_2 , NaOH or KOH . The impregnation process results in a porous structure of BAC available (Prauchner & Rodríguez-Reinoso, 2012). In addition, the main advantage of physical activation over chemical activation is that it avoids mixing impurities derived from the chemical activating agent (Şahin & Saka, 2013).

2.4 Antibacterial Properties of Carbon-Based Materials

2.4.1 Graphene Oxide Silver (GOAg)

Silver nanoparticles (AgNPs) serve as the most effective nano-agent against bacterial infections as they can be used in a variety of applications. AgNPs appear to have high potential in solving the multidrug resistance problem (often observed in bacterial strains) (Lozovskis et al., 2020). The drugs used to treat severe bacterial infections are progressively losing efficacy, resulting in unwanted effects. Hence, scientists have discovered that bacteria are less prone to developing resistance towards AgNPs than traditional antibiotics (Vi & Lue, 2016). The antibacterial properties of Ag have been utilized to preserve food and reduce wound infections. Silver has recently been incorporated into a variety of nanomaterials, including reduced graphene oxide (rGO), for the purpose of microbial disinfection (Chen, Li, & Chen, 2019).

Graphene oxide (GO) has recently gained popularity as a possible material for a variety of applications, including antibacterial (Vi & Lue, 2016). The antibacterial activity of GO has been attributed to membrane stress caused by the sharp edges (diamond sp³ type bonds characteristic) of GO nanosheets that might cause physical damage to cell membranes, resulting in bacterial membrane integrity loss. Graphene-functionalized antimicrobial nanoparticles have recently been used as promising antibacterial materials (Jaworski et al., 2018). The antimicrobial concept may be derived from GO confines bacteria while Ag kills them. The combination of GO and Ag NPs might be an efficient material due to its biocompatibility, simple synthesis and low cost (Vi & Lue, 2016). Antibacterial properties of GOAg towards *E. coli*, *S. aureus*, *S. epidermidis* and *C. albicans* have been studied. GOAg nanocomposite had the greatest

antibacterial effect against all tested microorganisms compared to GO and Ag alone. Bacterial cell growth treated with GOAg at 37 °C for 24 hours was greatly inhibited by 88.6%, 79.6%, 76.5% and 77.5% of *E. coli*, *S. aureus*, *S. epidermidis* and *C. albicans* respectively (Jaworski et al., 2018).

Multiple stages are involved in the antibacterial mechanism of GOAg. The first stage is GOAg dispersion into water. This stage involves the oxidation of AgNPs loaded on the GO sheets by dissolved oxygen to form stable aqueous colloids since GO sheets have a good hydrophilic affinity and aqueous dispersibility (Song et al., 2016). The second stage involves free Ag⁺ interaction with bacterial cells. Electrostatic attraction plays an important role at this stage, as negatively charged lipids on cell membranes where able to capture positively charged Ag⁺ easily (Song et al., 2016). The third stage involves silver ions disrupting the bacteria via binding membrane proteins or phospholipid bilayers. After the membrane system is destroyed, a huge amount of free Ag⁺, including GOAg nanocomposites, can enter the cells (Feng et al., 2000). The final stage involves Ag⁺ directly binding with proteins, lipids, enzymes and DNA and oxidizing them by generating excessive reactive oxygen species (ROS), which were mainly generated by the mitochondrial electron transport chain. ROS then oxidizes functional enzymes and disrupts the electron transport chain. This lead to the peroxidation of membrane lipid and oxidation of intracellular biomacromolecules, resulting in irreversible damage and, eventually, cell death (Song et al., 2016).

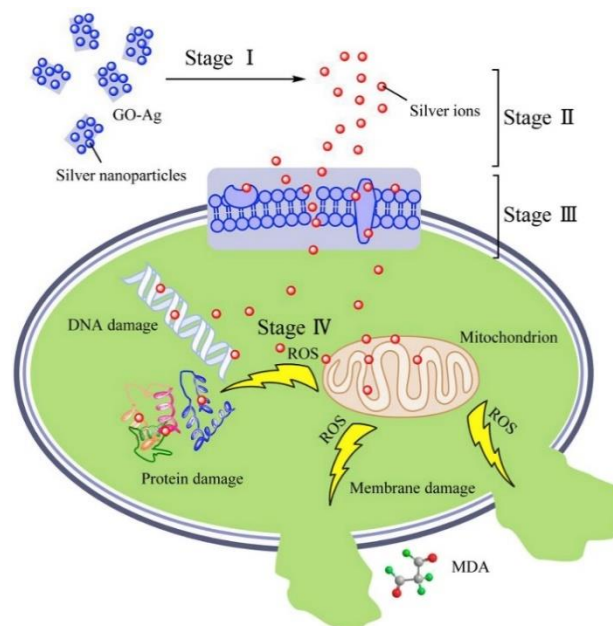


Figure 2.8: Schematic mechanisms of GOAg antibacterial behaviors (Song et al., 2016).

2.4.2 Bamboo Activated Carbon (BAC)

Unique antibacterial properties of bamboo derived from a bio-agent identified as "Kun" or "Kunh" (also known as "bamboo chinone"). In a direct translation, Kun represents a hydroxyl functional group ($-OH$) of bamboo. Moreover, bamboo Kun binds tightly to cellulose molecules throughout the bamboo fibre production process. Bamboo's antibacterial compound is 2, 6-dimethoxy-p-benzoquinone. In addition, bamboo has potent antibacterial properties, followed by bamboo grass (Afrin et al., 2009). Due to the presence of phenolic compounds in the chemical constituents of crude extracts of *Polygonum cuspidatum* roots (Mexican bamboo) demonstrate a wide range of antibacterial activities against Gram-positive and Gram-negative bacteria (Shan et al., 2008).

Afrin et al. (2012) conclude that the antibacterial agents of bamboo were located in lignin, making it a priority for wastewater/contaminated area cleaning. Lignin is a

complex network of polymers formed by oxidative coupling of three major phenylpropanoid units with many C – C and ether linkages. The antibacterial properties of bamboo may result from the presence of aromatic and phenolic functional groups in lignin. In addition, a 5% solution of bamboo extract (the lowest concentration) in water was enough to achieve a 100% sterilisation rate against *E. coli* (Afrin et al., 2012). While Tanaka et al. (2011) found that the antibacterial activity of Moso bamboo extract from shoot skins was effective against *S. aureus*. Furthermore, bamboo leaves extracts from bamboo manna were also found to have antibacterial activity against both Gram-positive and Gram-negative bacterial strains (Singh et al., 2019). Thus, these studies on various bamboo species have proven the antibacterial activity of bamboo. According to research, fibers extracted from bamboo culms were also discovered to have very high antibacterial properties (Tanaka et al., 2014).

2.5 Materials Characterization Technique

2.5.1 Morphological Study Using Field Emission Scanning Electron Microscope (FESEM)

FESEM is the abbreviation of Field Emission Scanning Electron Microscope. FESEM is a microscope that works with negatively charged particles which are electrons instead of light. These electrons are released from a field emission source. The specimen is scanned by the electron beam in a zigzag pattern on the scan coils (Information on the FESEM (Field-emission Scanning Electron Microscope), n. d.). FESEM has been used to study structures up to 1 nanometer in size as it provides topographical and elementary information at 10 to 300,000 times magnification with a practically unlimited depth of field. Other than that, FESEM provides clearer and less

electrostatically distorted images with a spatial resolution of up to 1 1/2 nanometers which is three to six times better than conventional Scanning Electron Microscopy (SEM) (Field emission scanning electron microscopy, 2021).

One of the main components of FESEM is the electron beam column. The column houses the field emitter gun (FEG), beam booster (deflector) and the electron magnetic lenses (condenser lens and objectives lens) (Figure 2.9). The design enables the smallest possible probe size for high-resolution images. The narrower the electron beam, the higher the resolution of imaging.

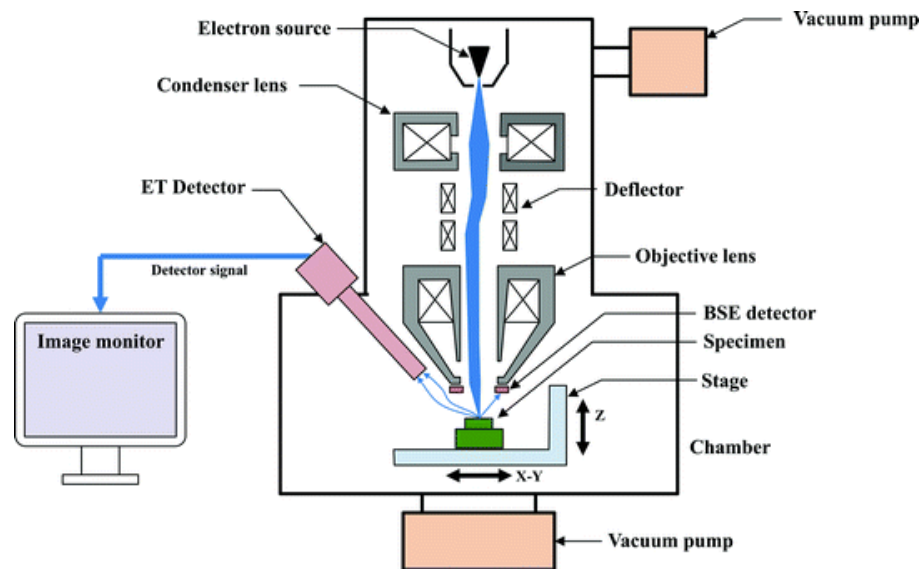


Figure 2.9: The electron beam column design of FESEM (Okano, 2018).

FESEM has been used to characterize the surface morphologies of carbon-based materials, including GOAg and BAC. The morphology of the AgNPs on GO nanosheets was more clearly observed using FESEM. Bao et al. (2011) not only found many white spots on the surface of the AgNP/GO composite paper that certainly AgNPs (uniformly distributed) but also within the networks of AgNP/GO composite paper as shown in Figure 2. 10 (B). Surface morphologies of BAC that were chemically activated by

using potassium hydroxide (KOH) were characterized using FESEM. Su et al. (2020) discovered the interior section of bamboo char (AC-Si) (Figure 2.11 (A)) was composed of microstructures and regular textured grooved structures with just few small sized pores (Figure 2.11 (B)).

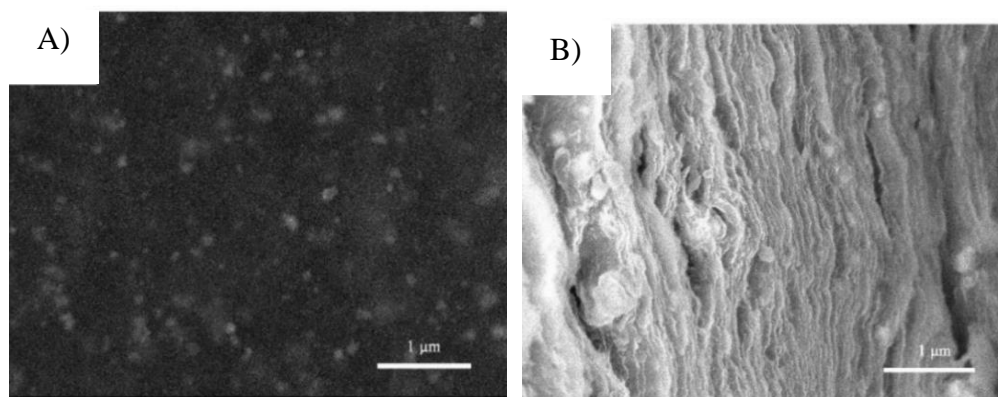


Figure 2.10: FESEM images from (A) Top-view of AgNP/GO composite paper; (B) Side-view of the cross sections of AgNP/GO composite paper (Bao et al., 2011).

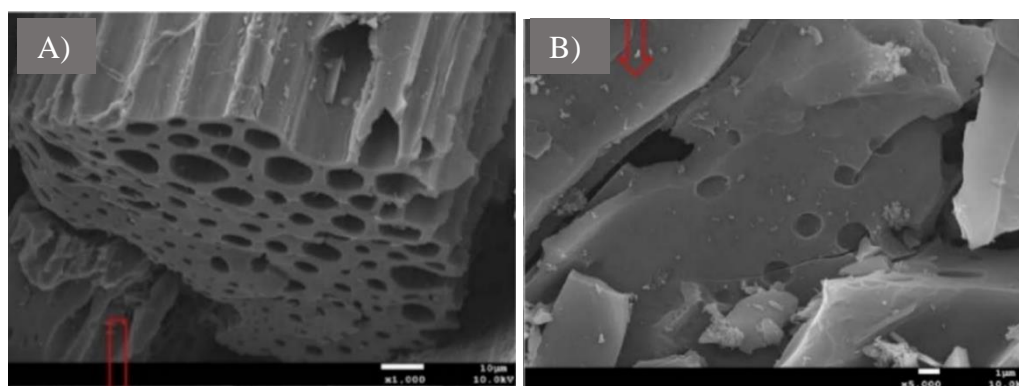


Figure 2.11: SEM images (A) Microstructure of AC-Si and (B) Regular textured grooved structure of AC-Si (Su et al., 2020).

2.5.2 Structural Analysis of Adsorbents Using X-ray Photoelectron Spectroscopy (XPS)

XPS is the abbreviation of X-ray photoelectron spectroscopy. XPS is a surface analysis technique it determines the energy distribution of photoelectrons produced by X-ray irradiating sample surfaces (Zou & Liu, 2020). Electron associated with XPS can